

Anisotropy and corotation of Galactic cosmic rays

M. Amenomori¹, S. Ayabe², X.J. Bi³, D. Chen⁴, S.W. Cui⁵,
 Danzengluobu⁶, L.K. Ding³, X.H. Ding⁶, C.F. Feng⁷, Zhaoyang Feng³,
 Z.Y. Feng⁸, X.Y. Gao⁹, Q.X. Geng⁹, H.W. Guo⁶, H.H. He³,
 M. He⁷, K. Hibino¹⁰, N. Hotta¹¹, Haibing Hu⁶, H.B. Hu³,
 J. Huang¹², Q. Huang⁸, H.Y. Jia⁸, F. Kajino¹³, K. Kasahara¹⁴,
 Y. Katayose⁴, C. Kato¹⁵, K. Kawata¹², Labaciren⁶, G.M. Le¹⁶,
 A.F. Li⁷, J.Y. Li⁷, Y.-Q. Lou¹⁷, H. Lu³, S.L. Lu³, X.R. Meng⁶,
 K. Mizutani^{2,18}, J. Mu⁹, K. Munakata¹⁵, A. Nagai¹⁹, H. Nanjo¹,
 M. Nishizawa²⁰, M. Ohnishi¹², I. Ohta²¹, H. Onuma², T. Ouchi¹⁰,
 S. Ozawa¹², J.R. Ren³, T. Saito²², T.Y. Saito¹², M. Sakata¹³,
 T.K. Sako¹², T. Sasaki¹⁰, M. Shibata⁴, A. Shiomi¹², T. Shirai¹⁰,
 H. Sugimoto²³, M. Takita¹², Y.H. Tan³, N. Tateyama¹⁰, S. Torii¹⁸,
 H. Tsuchiya²⁴, S. Udo¹², B. Wang⁹, H. Wang³, X. Wang¹²,
 Y.G. Wang⁷, H.R. Wu³, L. Xue⁷, Y. Yamamoto¹³, C.T. Yan¹²,
 X.C. Yang⁹, S. Yasue²⁵, Z.H. Ye¹⁶, G.C. Yu⁸, A.F. Yuan⁶,
 T. Yuda¹⁰, H.M. Zhang³, J.L. Zhang³, N.J. Zhang⁷, X.Y. Zhang⁷,
 Y. Zhang³, Yi Zhang^{3*}, Zhaxisangzhu⁶, and X.X. Zhou⁸

(The Tibet AS γ Collaboration)

*To whom correspondence should be addressed; E-mail: zhangyi@mail.ihep.ac.cn

1. Department of Physics, Hirosaki University, Hirosaki 036-8561, Japan
2. Department of Physics, Saitama University, Saitama 338-8570, Japan
3. Key Laboratory of Particle Astrophysics, Institute of High Energy Physics, Chinese Academy of Sciences, Beijing 100049, China
4. Faculty of Engineering, Yokohama National University, Yokohama 240-8501, Japan
5. Department of Physics, Hebei Normal University, Shijiazhuang 050016, China
6. Department of Mathematics and Physics, Tibet University, Lhasa 850000, China

7. Department of Physics, Shandong University, Jinan 250100, China
8. Institute of Modern Physics, South West Jiaotong University, Chengdu 610031, China
9. Department of Physics, Yunnan University, Kunming 650091, China
10. Faculty of Engineering, Kanagawa University, Yokohama 221-8686, Japan
11. Faculty of Education, Utsunomiya University, Utsunomiya 321-8505, Japan
12. Institute for Cosmic Ray Research, University of Tokyo, Kashiwa 277-8582, Japan
13. Department of Physics, Konan University, Kobe 658-8501, Japan
14. Faculty of Systems Engineering, Shibaura Institute of Technology, Saitama 337-8570, Japan
15. Department of Physics, Shinshu University, Matsumoto 390-8621, Japan
16. Center of Space Science and Application Research, Chinese Academy of Sciences, Beijing 100080, China
17. Physics Department and Tsinghua Center for Astrophysics, Tsinghua University, Beijing 100084, China
18. Advanced Research Institute for Science and Engineering, Waseda University, Tokyo 169-8555, Japan
19. Advanced Media Network Center, Utsunomiya University, Utsunomiya 321-8585, Japan
20. National Institute of Informatics, Tokyo 101-8430, Japan
21. Tochigi Study Center, University of the Air, Utsunomiya 321-0943, Japan
22. Tokyo Metropolitan College of Industrial Technology, Tokyo 116-8523, Japan
23. Shonan Institute of Technology, Fujisawa 251-8511, Japan
24. RIKEN, Wako 351-0198, Japan
25. School of General Education, Shinshu University, Matsumoto 390-8621, Japan

The intensity of Galactic cosmic rays is nearly isotropic due to the influence of magnetic fields in the Milky Way. Here we present two-dimensional high-precision anisotropy measurement for energies from a few to several hundred TeV using the huge data sample of the Tibet Air Shower Arrays. Besides revealing finer details of the known anisotropies, a new component of sidereal time Galactic cosmic ray anisotropy is uncovered around the Cygnus region direction. For cosmic-ray energies up to a few hundred TeV, all components of anisotropies fade away, showing a corotation of Galactic cosmic rays with the local Galactic magnetic environment. These results bear broad implications to cosmic rays, supernovae, magnetic field, heliospheric and Galactic dynamic environment in a comprehensive manner.

Galactic cosmic rays

The anisotropy of Galactic cosmic rays (GCRs) may result from an uneven distribution of cosmic ray (CR) sources and the process of CR propagation in the Milky Way. CRs of energy below 10^{15} eV are accelerated by diffusive magnetohydrodynamic (MHD) shocks (1, 2, 3, 4) of supernova remnants (SNRs) and stellar winds. The discreteness of SNRs could lead to a CR anisotropy (5). However, GCRs must almost completely lose their original directional information; their orbits are deflected by the Galactic magnetic field (GMF) and are randomized by irregular GMF components, having traveled on average for many millions of years, some also having interacted with interstellar gas atoms and dusts. The transport of CRs in a magnetized plasma is governed by four major processes: convection, drift, anisotropic diffusion and adiabatic energy change (deceleration or acceleration) (6, 7). High-precision measurement of the CR anisotropy provides a means to explore magnetic field structures and gains insight for the CR transport parameters (8). The long-term high-altitude observation at the Tibet Air Shower Arrays (referred to as the Tibet AS γ experiment) has accumulated tens of billions of CR events in the multi-TeV energy range, ready for an unprecedented high-precision measurement of the CR anisotropy as well as the temporal and energy dependence of the CR anisotropy.

An expected anisotropy is caused by the relative motion between the observer and the CR plasma, known as the Compton-Getting (CG) effect (9) with CRs arriving more intense from the motion direction and less intense from the opposite direction. Such a CR anisotropy, caused by the Earth orbital motion around the Sun, has indeed been detected (10, 11). Data assembled to 1930s (9) were consistent with a scenario that the CR plasma stays at rest in an inertial frame of reference attached to the Galactic center. If this were true, the Galactic rotation in the solar neighborhood might then be measurable. Nevertheless, such CR anisotropy due to the solar system rotation around the Galactic center at a speed of $\sim 220 \text{ km s}^{-1}$ remained inconclusive

over seven decades. Now our high-precision two-dimensional (2D) measurement gives a strong evidence to exclude the CR anisotropy of this origin and thus show a corotation of GCRs with the local GMF environment.

Historically, the GCR anisotropy (12, 13) has been measured as the sidereal time variation at the spinning Earth using both underground μ detectors and ground-based air shower arrays (14, 15, 16, 17, 18, 19). Located at different geographical latitudes and operating in different years with various threshold energies, each individual experiment could only measure the CR modulation profile along the R.A. direction which was usually fitted by first few harmonics. Instead of using sine or cosine harmonics, one may adopt two Gaussian functions with Declination dependent parameters (mean, width and amplitude) to fit the so-called “tail-in” and “loss-cone” features, and a tentative 2D anisotropic picture was obtained (20, 21) by simultaneously fitting different experimental data. Here, the CR deficiency was thought to be associated with a magnetic cone-like structure and thus the name ‘loss-cone’, while the CR enhancement is roughly in the direction of the heliospheric magnetotail and is thus referred to as ‘tail-in’ enhancement (12, 13). However, the accurate spatial and energy dependence of CR anisotropy could not be given (22), and some subtle features remain hard to reveal, since the CR anisotropy is more complex and cannot be properly described by two Gaussians. The Tibet AS- γ experiment alone can achieve 2D measurement in various energy ranges and to provide details of the 2D CR anisotropy.

Tibet Air Shower Array Experiment

The Tibet Air Shower Array experiment has been conducted at Yangbajing (90.522 E, 30.102 N; 4300 m above the sea level) in Tibet, China since 1990. The Tibet I array (23), consisting of 49 scintillation counters and forming a 7×7 matrix of 15 m span, was expanded to become the Tibet II array with an area of 36,900 m² by increasing the number of counters in 1994. In 1996,

part of Tibet II with an area of 5175 m^2 was upgraded to a high-density (HD) array with a 7.5 m span (24). To increase the event rate, the HD array was enlarged in 1999 to cover the central part of Tibet II as Tibet III array (25, 26, 27). The area of Tibet III array has reached $22,050 \text{ m}^2$. The trigger rates are $\sim 105\text{Hz}$ and $\sim 680\text{Hz}$ for the Tibet HD and III arrays, respectively. The data were acquired by running the HD array for 555.9 live days from 1997.2 to 1999.9 and the Tibet III array for 1318.9 live days from 1999.11 to 2005.10. GCR events are selected, if any four-fold coincidence occurs in the counters with each recording more than 0.8 particles in charge, the air shower core position is located in the array and the zenith angle of arrival direction is $\lesssim 40^\circ$. With all those criteria, both Tibet HD and III arrays have the modal energy of 3 TeV and a moderate energy resolution; the $\sim 0.9^\circ$ angular resolution estimated from Monte Carlo simulations (28, 29) was verified by the Moon shadow measurement (25, 26, 27). In total, ~ 37 billion CR events are used in our data analysis.

Data analysis and results

With such a large data sample, we conduct a 2D measurement to reveal detailed structural information of the large-scale GCR anisotropy beyond the simple R.A. profiles. For each short time step (e.g. 2 minutes), the relative CR intensity at points in each zenith angle belt can be compared and this comparison can be extended step by step to all points in the surveyed sky [see Refs. (30) for details of data analysis]. Lacking the absolute detector efficiency calibration in the Dec direction, absolute CR intensities along different Dec directions cannot be compared. Thus, the average intensity in each narrow Dec belt is normalized to unity. Our analysis procedure would give a correct 2D anisotropy if there is no variation in the average CR intensity for different Dec. We systematically examined the CR anisotropy in four different time frames, namely solar time for solar modulation, sidereal time for Galactic modulation, anti-sidereal time and extended-sidereal time; and systematic variations are found to be unimportant.

To study the temporal variation of CR modulation, we divide the data sample into two subsets. The first subset is from 1997.2 to 2001.10 covering the 23rd solar maximum (a period of a few years when solar magnetic activity are the strongest) while the second subset is from 2001.12 to 2005.11 approaching the solar minimum (a period of a few years when solar magnetic activity become minimal). Comparing the sidereal time plots for these two intervals (Fig. 1) shows that the CR anisotropy is fairly stable and insensitive to solar activity. The ‘tail-in’ and ‘loss-cone’ anisotropy components (*12, 13*), extracted earlier from a combination of the underground μ telescope data analyses (*20, 21*), are seen in our 2D plots in much finer details and with a high significance (Fig. 1). Our new high-precision measurement thus provides constraints on physical interpretations of these features.

Spreading across $\sim 280^\circ$ to $\sim 360^\circ$ in R.A., a new excess component with a $\sim 0.1\%$ increase of the CR intensity peaked at Dec $\sim 38^\circ$ N and R.A. $\sim 309^\circ$ in the Cygnus region is detected at a high significance level of 13.3σ with a 5° pixel radius (Fig. 1d). The Cygnus region, where complex features are revealed in broad wavelength bands of radio, infrared, X-ray and gamma-rays, is rich of candidate GCR sources. Recently, the first unidentified TeV gamma-ray source was discovered here by HEGRA (*31*). This region, as observed by EGRET (*32*), appears to be the brightest source of diffuse GeV gamma-rays in the northern sky and contributes significantly to the diffuse TeV gamma-ray emission in the Galactic plane as observed by Milagro (*33*) which rejects 90% of CR background while still retains $\sim 45\%$ of gamma-rays. Such gamma-rays originate from the interaction of CRs with gas and dusts. Using more stringent event selection criteria (*30*), a deeper view of Cygnus region with a 0.9° pixel radius shows that the large-scale excess consists of a few spatially separated excesses of smaller scales superposed onto a large-scale anisotropy (Fig. 1e); these small-scale ($\sim 2^\circ$) excess favors the interpretation that the extended gamma-ray emission from the Cygnus region contributes significantly to the overall excess in the region (*34*). As our experiment cannot yet distinguish gamma-rays

from the charged CR background, we cannot tell how much of this excess is to be attributed to gamma-rays and how much, if any, is associated with charged CRs (35). Such a determination requires upgrading the Tibet arrays for CR and gamma-ray discrimination.

The solar time CR modulation was also stable (Fig. 2). We found that including events with fewer than 8 detector coincidences (lower energy events) resulted in much larger modulation amplitudes than those obtained when these events were excluded (higher energy events). To avoid this, high multiplicity events with coincident detector numbers ≥ 8 were adopted (Fig. 2). The observed dipole anisotropy agrees very well with the expected CG effect due to the Earth orbital motion around the Sun. Thus, heliospheric magnetic field and solar activity does not influence the multi-TeV CR anisotropy.

Because of the stable nature of the sidereal time modulation, data from different years were combined to examine the energy dependence of CR anisotropy. Fig. 3 shows the variation of anisotropy for five groups of events according to their different primary energies. For primary energies below 12 TeV, the anisotropies show little dependence on energy while above this energy, anisotropies fade away, consistent with a CR isotropy of KASCADE (17) in the energy range of 0.7 – 6PeV. Contrary to the earlier suggestion (13), the ‘tail-in’ component remains still visible above 50 TeV in smaller regions. Since the multi-TeV GCRs, whose gyro-radii are hundreds or thousands of AUs, are not affected by the heliospheric magnetic field, it is clear that the GMF must be responsible for both ‘tail-in’ and ‘loss-cone’ modulations.

As a result of a diminishing GCR anisotropy at high energies, we can test the CG anisotropy caused by the orbital motion of the solar system in our Galaxy, which would peak at ($\alpha = 315^\circ$, $\delta = 49^\circ$) and minimize at ($\alpha = 135^\circ$, $\delta = -49^\circ$) with an amplitude of 0.35%. This would be a salient signal in a real 2D measurement. However, as explained earlier, the modulation along the Dec direction is partly lost. After applying the normalization procedure along each Dec belt, the expected CG anisotropy is distorted and apparently peaks at ($\alpha = 315^\circ$, $\delta = 0^\circ$)

and forms a trough around ($\alpha = 135^\circ$, $\delta = 0^\circ$) with a smaller amplitude of $\sim 0.23\%$ (Fig. 4). To avoid any contamination from the non-vanishing ‘tail-in’ and ‘loss-cone’ anisotropies (12, 13) when the primary energy is of ~ 300 TeV, the upper half of the surveyed CR intensity map (with $\text{Dec} > 25^\circ$) is used to compare with the predicted Galactic CG effect of an amplitude $\sim 0.16\%$. The fitted anisotropy amplitude is $0.03\% \pm 0.03\%$, consistent with an isotropic CR intensity. Therefore our observation exclude the existence of the Galactic CG effect with a high-degree confidence, assuming the absence of other cancelling effects. The null result of the Galactic CG effect implies that GCRs corotate with the local GMF environment.

Discussion

The observation of GCR anisotropy and diffuse gamma-ray emission plays an important role in probing sources and propagation of CRs. The detection of the new large-scale GCR anisotropy component and the indication of extended gamma-ray emission from the same mysterious Cygnus region allow us to connect the GCR acceleration site and propagation. A precision spectral and morphological determination of the extended gamma-ray emission would be our next pursuit. The existence of large-scale GCR anisotropies up to a few tens of TeV indicates that they are not related to the heliospheric magnetic field. It is conceivable that GMF has large-scale structures in the heliospheric neighborhood.

As in many spiral galaxies, our Milky Way has large-scale differential rotations in stellar and magnetized gas disks with a GMF of a few micro Gauss. The GMF, GCRs and thermal gas have similar energy densities of $\sim 1\text{eV cm}^{-3}$ and interact with each other dynamically. The corotation of the GCR plasma with the local GMF environment around the Galactic center is enforced by the Lorentz force as GCRs randomly scatter and drift in irregular GMF components (36). As the Galactic disk rotates differentially, the important inference is that the bulk GCR plasma within and above the Galactic disk must also rotate differentially. The GCR coro-

tation evidence provides an important empirical basis for the study of galactic MHD processes, such as modeling synchrotron emission diagnostics for large-scale spiral structures of MHD density waves (37, 38, 39).

References and Notes

1. H. J. Voelk, in *Frontiers of Cosmic Ray Science*, T. Kajita, Y. Asaoka, A. Kawachi, Y. Matsumura, M. Sasaki, Eds. (Universal Academy Press, Tokyo, 2003) pp.29-48.
2. Y.-Q. Lou, *Astrophys. J. Lett.* **428**, L21 (1994).
3. A. Dar, *Nuovo Cim. B* **120**, 767 (2005).
4. C. Yu, Y.-Q. Lou, F. Y. Bian, Y. Wu, *Mon. Not. Roy. Astron. Soc.* **370**, 121 (2006).
5. A. D. Erlykin, A. W. Wolfendale, *Astropart. Phys.* **25**, 183 (2006).
6. G. F. Krymsky, *Geomagn. Aeron.* **977**, 763 (1964).
7. E. N. Parker, *Planet. Space Sci.* **13**, 9 (1965).
8. B. Heber, in *Proc. 27th Int. Cosmic Ray Conf.*, M.Simon, E.Lorenz, M.Pohl Eds., Invited, Rapporteur and Highlighted papers (CDROM, 2002) pp.118-135.
9. A. H. Compton, I. A. Getting, *Phys. Rev.* **47**, 817 (1935).
10. D. J. Cutler, D. E. Groom, *Nature* **322**, L434 (1986).
11. M. Amenomori *et al.*, *Phys. Rev. Lett.* **93**, 061101 (2004).
12. K. Nagashima, S. Mori, in *Proc. Int. Cosmic Ray Symp. on High Energy Cosmic Ray Modulation*, Univ. of Tokyo, Tokyo, Japan, 326 (1976).

13. K. Nagashima, K. Fujimoto, R. M. Jacklyn, *J. Geophys. Res.* **103**, 17429 (1998).
14. K. Munakata *et al.*, *Phys. Rev. D***56**, 23 (1997).
15. M. Ambrosio *et al.*, *Phys. Rev. D***67**, 042002 (2003).
16. M. Aglietta, *et al.*, in *Proc. 28th Int. Cosmic Ray Conf.*, T. Kajita, Y. Asaoka, A. Kawachi, Y. Matsubara, M. Sasaki, Eds., (Universal Academy Press, Tokyo, 2003) **4**, pp.183-186.
17. T. Antoni *et al.*, *Astrophys. J.* **604**, 687 (2004).
18. G. Guillian *et al.*, *Phy. Rev. D*, in press (see <http://arxiv.org/astro-ph/0508468>).
19. M. Amenomori *et al.*, *Astrophys. J.* **626**, L29 (2005).
20. D. L. Hall *et al.*, *J. Geophys. Res.* **103**, 367 (1998).
21. D. L. Hall *et al.*, *J. Geophys. Res.* **104**, 6737 (1999).
22. M. L. Duldig, *PASA*, **18(1)**, 12 (2001).
23. M. Amenomori *et al.*, *Phys. Rev. Lett.* **69**, 2468 (1992).
24. M. Amenomori *et al.*, in *International Symposium on High Energy Gamma-Ray Astronomy*, F.A. Aharonian, H.J. Voelk Eds. (AIP Conference Proceedings 558, 2001), pp.557-564.
25. M. Amenomori *et al.*, *Proc. 27th Int. Cosmic Ray Conf.*, M.Simon, E.Lorenz, M. Pohl Eds. (Copernicus Gesellschaft, 2002), **2**, pp.573-576.
26. M. Amenomori *et al.*, *Phy. Rev. D***47**, 2675 (1993).
27. M. Amenomori *et al.*, *Astrophys. J.* **598**, 242 (2003).
28. M. Amenomori *et al.*, *Nucl. Instrum. Methods Phys. Res. A***288**, 619 (1990).

29. K. Kasahara, <http://cosmos.n.kanagawa-u.ac.jp/EPICSHome/>
30. M. Amenomori *et al.*, *Astrophys. J.* **633**, 1005 (2005).
31. F. A. Aharonian *et al.*, *A & A* **393**, L37 (2002).
32. S. D. Hunter *et al.*, *Astrophys. J.* **481**, 205 (1997).
33. R. Atkins *et al.*, *Phys. Rev. Lett.* **95**, 251103 (2005).
34. G. Walker, R. Atkins, D. Kieda, *Astrophys. J.* **614**, L93 (2004).
35. L. Bergamasco *et al.*, in *Proc. 21th Int. Cosmic Ray Conf. (Adelaide)*, **6**, 372-375 (1990).
36. E. N. Parker, *Astrophys. J.* **145**, 811 (1966).
37. Z. H. Fan, Y.-Q. Lou, *Nature* **383**, 800 (1996).
38. Y.-Q. Lou, Z. H. Fan, *Mon. Not. Roy. Astron. Soc.* **341**, 909 (2003).
39. Y.-Q. Lou, X. N. Bai, *Mon. Not. Roy. Astron. Soc.* in press (2006; astro-ph/0607328).
40. The collaborative experiment of the Tibet Air Shower Arrays has been under the auspices of the Ministry of Science and Technology of China and the Ministry of Foreign Affairs of Japan. This work was supported in part by Grants-in-Aid for Scientific Research on Priority Areas (712) (MEXT), by Scientific Research (JSPS) in Japan, by the National Natural Science Foundation of China and by the Chinese Academy of Sciences. The authors thank J. Kóta for reading the manuscript and critical comments.

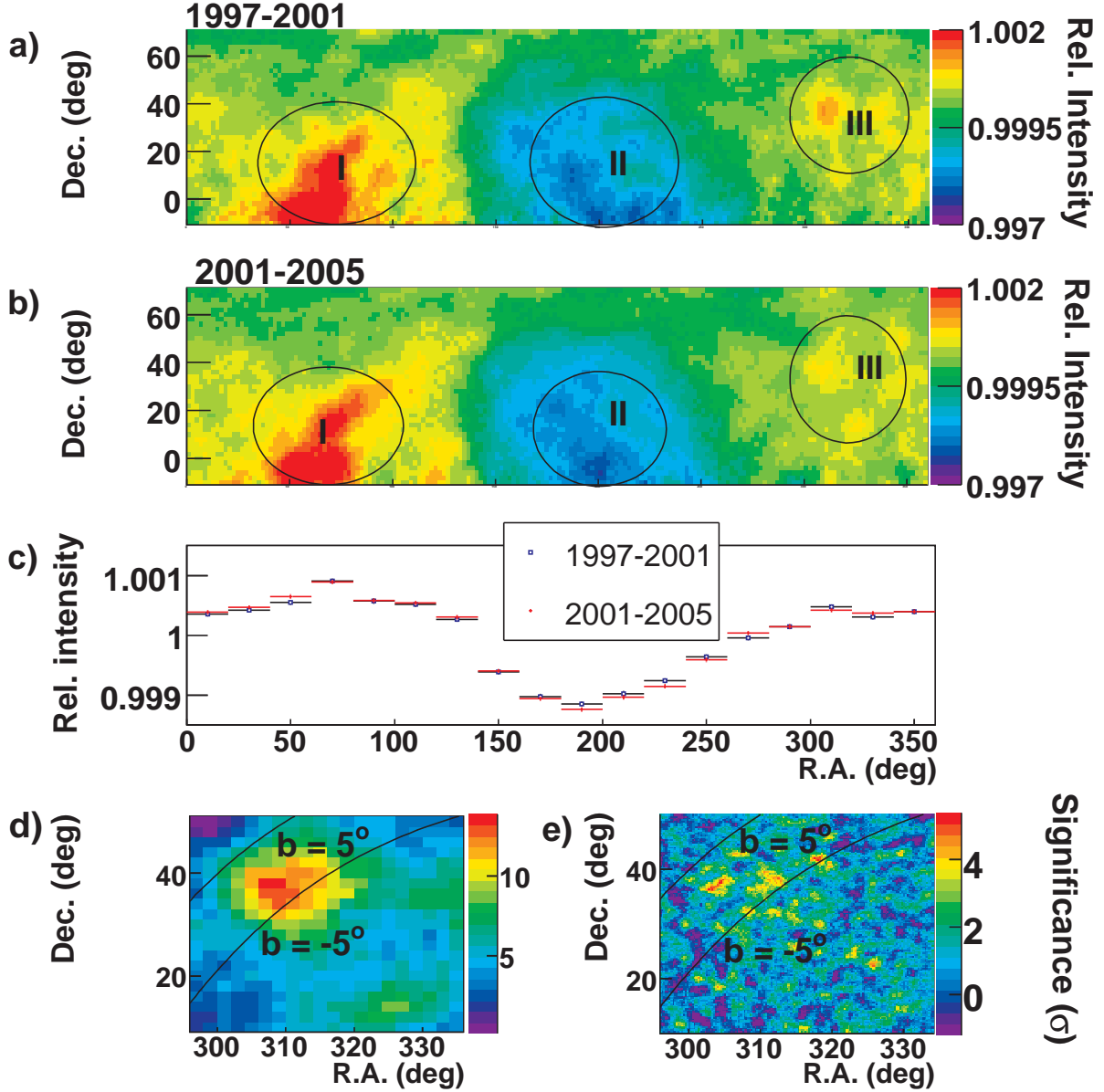


Figure 1: Celestial CR intensity map[†] for Tibet AS γ data taken from 1997–2001 (a) and 2001–2005 (b). The vertical color bin width is 2.5×10^{-4} for the relative intensity in both (a) and (b). The circled regions labeled by I, II and III are the ‘tail-in’, ‘loss-cone’ (I_2 , I_3) and newly found anisotropy component around the Cygnus region ($\sim 38^\circ$ N Dec and $\sim 309^\circ$ R.A.), respectively. Panel (c) is the one-dimensional (1D) projection of the 2D maps in R.A. for comparison. Panels (d) and (e) show the significance maps of Cygnus region (pixels in radius of 0.9° and sampled over a square grid of side width 0.25° for (e)) for data of 1997–2005. The vertical color bin widths are 0.69σ and 0.42σ for the significance in (d) and (e), respectively. Two thin curves in both (d) and (e) stand for the Galactic parallel $b = \pm 5^\circ$. Small-scale anisotropies (e) superposed onto the large-scale anisotropy hint at the extended gamma-ray emission. [†]Unless otherwise stated, images in Figs 1–4 are presented using pixels in radius of 5° and sampled over a square grid of side width 2° ; the modal energy is 3 TeV.

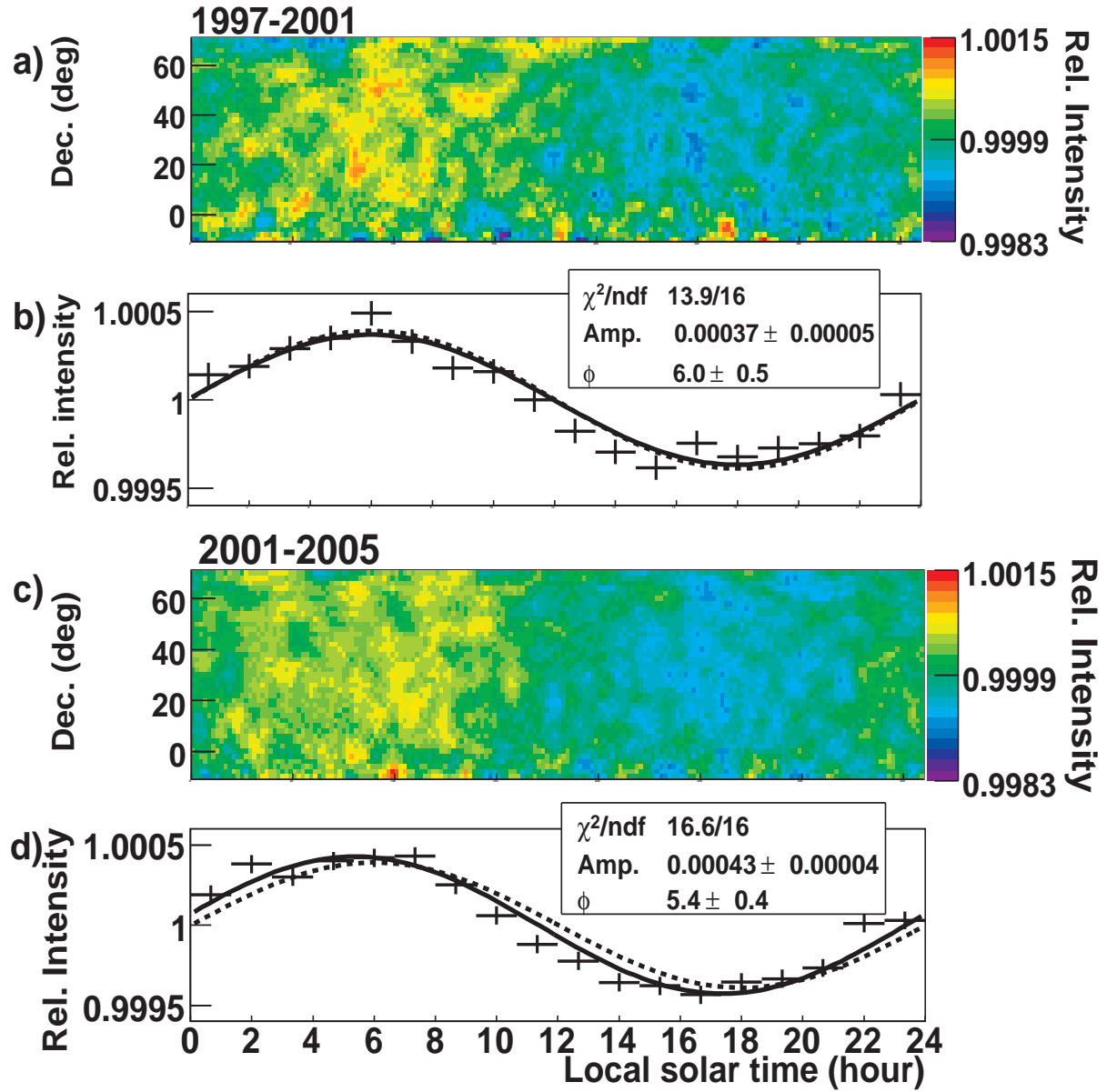


Figure 2: Local solar time CR intensity map for the Tibet AS γ data taken from 1997–2001 (a) and (b) and 2001–2005 (c) and (d). Both samples have the modal energy of 10 TeV. The vertical color bin width is 1.6×10^{-4} for the relative intensity in both (a) and (c). In both (b) and (d), the fitting function is in the form of $\text{Amp} * \cos[2\pi(T-\phi)/24]$ where the local solar time T and ϕ are in unit of hour and Amp is the amplitude. The χ^2 fit involves the number of degree of freedom (ndf) given by the number of bins minus 2 due to the two fitting parameters Amp and ϕ . The 1D plots are the projection of the 2D maps in local solar time. In the 1D plots the dashed lines are from the expected CG effect, while the solid lines are the best harmonic fits, which agree very well with the prediction. The solar time modulation appears quite stable and insensitive to solar activity.

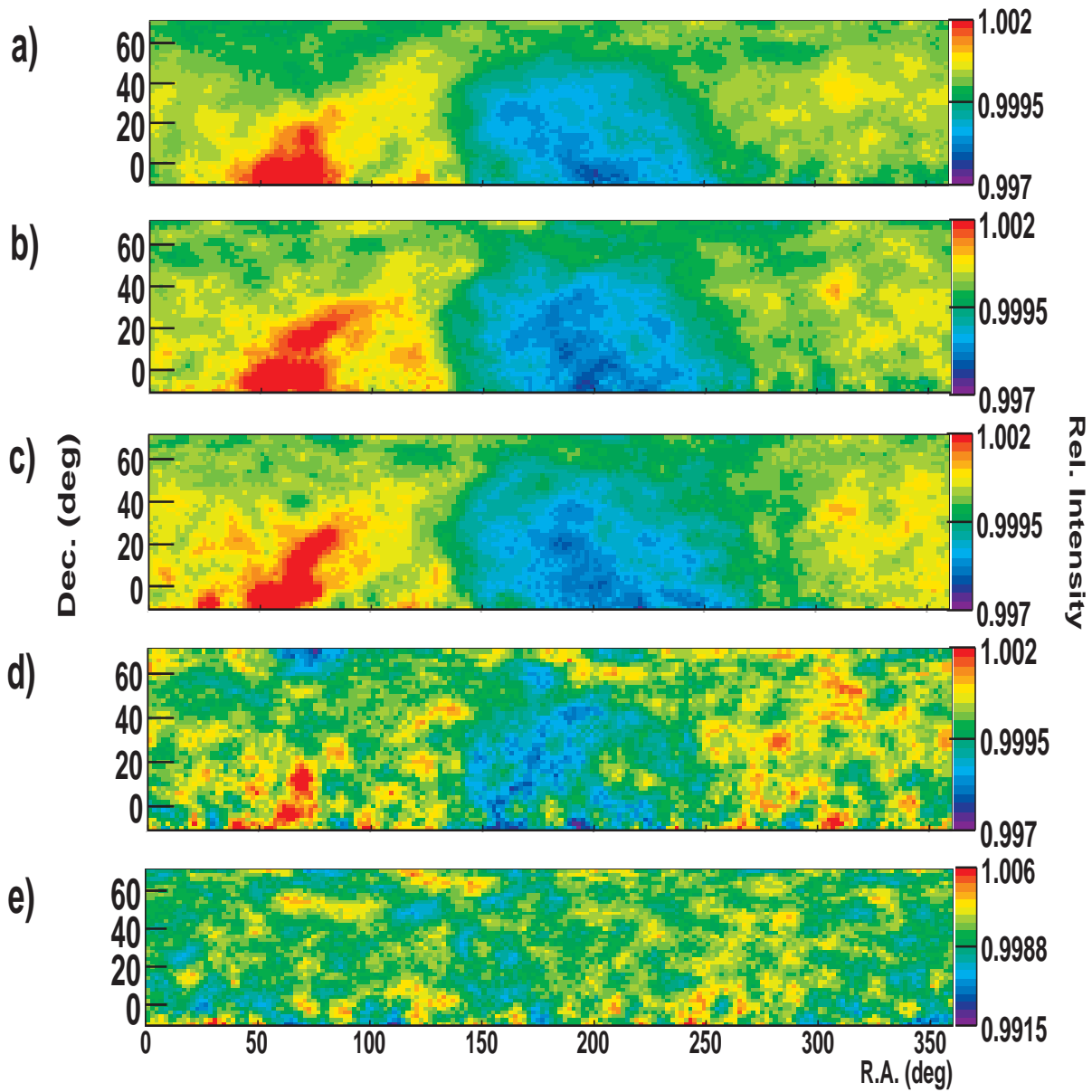


Figure 3: Celestial CR intensity map for different representative CR energies: (a) 4 TeV; (b) 6.2 TeV; (c) 12 TeV; (d) 50 TeV; (e) 300 TeV. Data were taken during 1997–2005. The vertical color bin width is 2.5×10^{-4} in (a)–(d), while it is 7.25×10^{-4} in (e) for different statistics, all for the relative CR intensity.

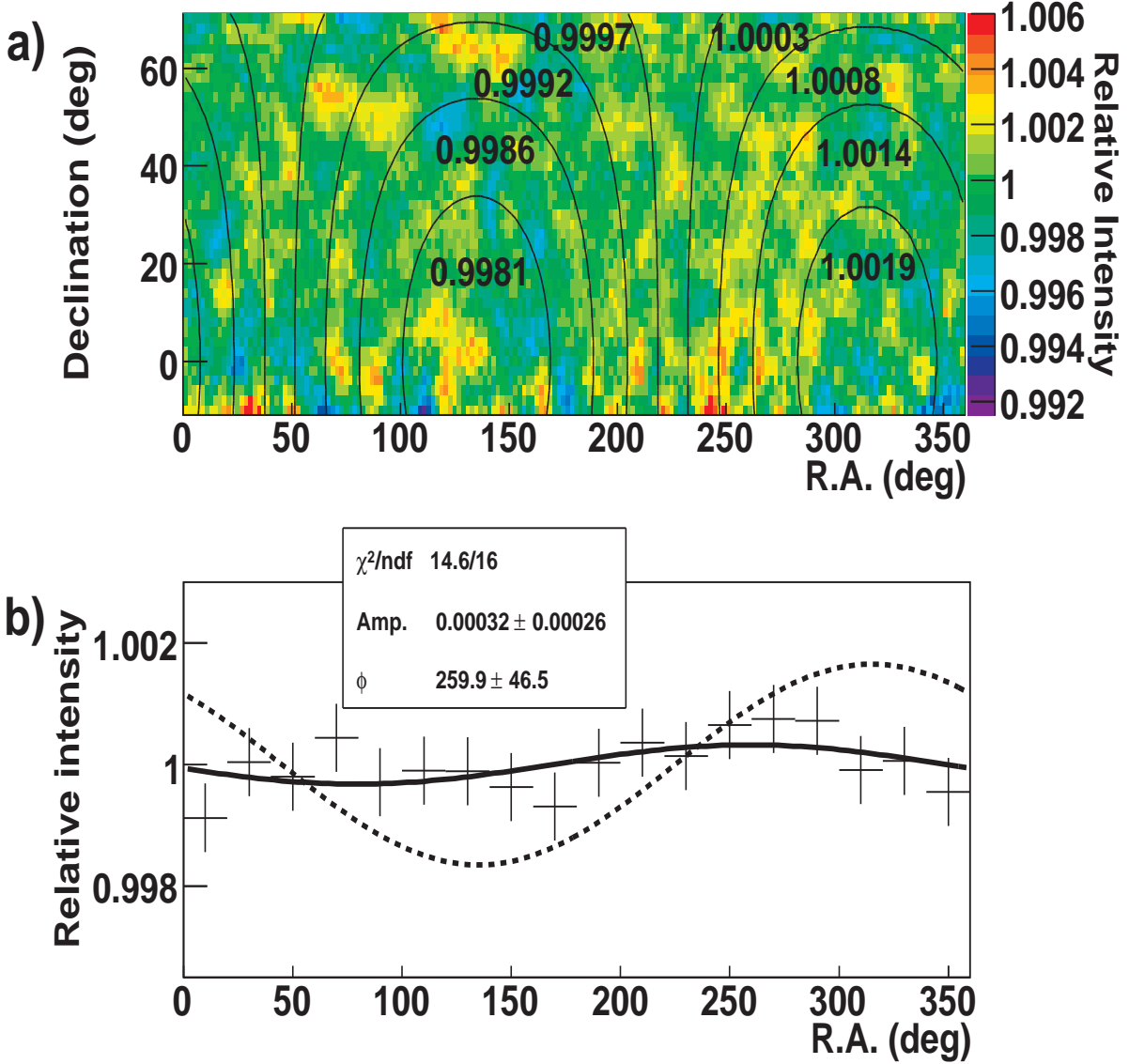


Figure 4: Celestial or 2D local sidereal time CR intensity map and its 1D projection in the R.A. direction for 300 TeV CRs of all data. (a) The colored map is the same as Fig. 3e, while the contours are the “apparent” 2D anisotropy expected from the Galactic CG effect. The vertical color bin width is 7.25×10^{-4} for the relative intensity in (a). The 1D projection is in map (b) for Dec between $25^\circ - 70^\circ$, where the dashed line is the expected Galactic CG response while the solid line is the best fit to this observation using a first-order harmonic function. The fitting function is in the form of $\text{Amp} * \cos(\text{R.A.} - \phi)$ where ϕ is in degree and Amp is the amplitude. The χ^2 fit involves the ndf given by the number of bins minus 2 for the two fitting parameters Amp and ϕ . The data shows no Galactic CG effect with a high-level of confidence.